Structure of Zirconium-Exchanged H-ZSM5 Prepared by Vapor Exchange of $ZrCl_4$

Howard S. Lacheen and Enrique Iglesia*

Department of Chemical Engineering, University of California at Berkeley, Berkeley, California 94720

Received February 24, 2006. Revised Manuscript Received January 21, 2007

Zr dimers ($Zr_2O_3^{2+}$) interacting with two exchange sites and uniform in structure were prepared by grafting anhydrous $ZrCl_4$(g) onto H-ZSM5 followed by hydrolysis and dehydration. This method led to selective exchange, without concurrent formation of crystalline ZrO_2 aggregates, ubiquitously formed via aqueous exchange because of the slow diffusion of aquo oxo-ions within small channels. $ZrCl_4$(g) reacts with acidic OH groups to form HCl and $ZrCl_3^+$-ZSM5 species. This exchange stoichiometry was confirmed by the number of HCl molecules evolved during hydrolysis, a process that forms $ZrO(OH)^+$ species. These species then dehydroxylate via condensation with vicinal $ZrO(OH)^+$ to form $(O{=}Zr{-}O{-}Zr{=}O)^{2+}$ species interacting with two exchange sites and containing one bridging O-atom. This exchange process is consistent with the number of residual OH groups titrated by D_2 and with the intensity of O−H infrared bands. X-ray diffraction, ^{27}Al nuclear magnetic resonance, and infrared spectra showed that the exchange process did not influence zeolite crystallinity, led to Zr^{4+} introduction into the zeolite framework, or form residual $Zr(OH)_x$ species at exchange sites. Weak Raman bands in the 960−1030 cm^{-1} region, absent in crystalline ZrO_2 and H-ZSM5, were detected upon exchange. The maximum attainable Zr_{dimer}/Al_f exchange ratios (0.6 ± 0.05) are consistent with Al radial structure distributions and with expected Al−Al distances required to anchor $(O{=}Zr{-}O{-}Zr{=}O)^{2+}$ species in ZSM-5 with a statistical distribution of Al atoms. $ZrCl_4$ species in excess of this saturation stoichiometry formed monoclinic ZrO_2, detectable in Raman spectra and X-ray diffraction patterns.

1. Introduction

Cations exchanged onto microporous solids have been widely studied[1−7] because they can introduce sites active in redox cycles and C−H bond activation.[6,8−10] Aqueous media are effective for the exchange of monovalent and divalent cations into 8-ring and 10-ring zeolites.[7,11−13] High-valent cations (M^{n+}, $n > 2$) form highly charged solvated oligomers in aqueous media and these species diffuse slowly into zeolite channels containing the exchange sites.[14] Alternate strategies have exploited volatile oxides (MoO_3),[15] halides[16] ($FeCl_3$, WCl_6),[9,17] or carbonyls ($Mo(CO)_6$),[18] which form small neutral precursors in the gas phase.

Zirconium silicates ($Zr_xSi_{1-x}O_2$) have been reported to form for several zeolite structures prepared by hydrothermal methods together with Zr^{4+} cations at framework positions (from infrared Zr−O−Si stretches at 940−960 cm^{-1}; assigned by analogy with TS-1)[19−22] and expanded unit cells (from X-ray diffraction).[19−21] Postsynthesis exchange of Zr^{4+}-oxo cations onto medium-pore Al-containing zeolites, however, has not been conclusively demonstrated. Exchange of [Al]-ZSM-5 with aqueous $ZrOCl_2$ introduced only trace levels of Zr ($Zr/Al < 0.06$), indicating that Zr^{4+}-oxo species in aqueous media did not diffuse into 10-ring zeolite channels.[12] Isolated Zr-oxo species at exchange sites are likely to show adsorption and catalytic functions different from crystalline ZrO_2 or $Zr_xSi_{1-x}O_2$. ZrO_x species grafted onto SiO_2 have been reported as active photocatalysts for CH_4 coupling[23] and ZrO_x species prepared by impregnation

* To whom correspondence should be addressed. E-mail: iglesia@cchem.berkeley.edu.

(1) Schreier, M.; Teren, S.; Belcher, L.; Regalbuto, J. R.; Miller, J. T. *Nanotechnology* **2005**, *16*, S582.
(2) Wang, H.; Su, L.; Zhuang, J.; Tan, D.; Xu, Y.; Bao, X. *J. Phys. Chem. B* **2003**, *107*, 12964.
(3) Viswanadham, N.; Shido, T.; Sasaki, T.; Iwasawa, Y. *Sci. Tech. Catal.* **2002**, *35*, 189.
(4) Viswanadham, N.; Shido, T.; Iwasawa, Y. *Appl. Catal., A* **2001**, *219*, 223.
(5) Solsona, B.; Blasco, T.; López Nieto, J. M.; Peña, M. L.; Rey, F.; Vidal-Moya, A. *J. Catal.* **2001**, *203*, 443.
(6) Shu, Y.; Ichikawa, M. *Catal. Today* **2001**, *71*, 55.
(7) Li, W.; Yu, S. Y.; Meitzner, G. D.; Iglesia, E. *J. Phys. Chem. B* **2001**, *1005*, 1176.
(8) Kim, Y.-H.; Borry, R. W.; Iglesia, E. *Microporous Mesoporous Mater.* **2000**, *35*, 495.
(9) Ding, W.; Meitzner, G. D.; Marler, D. O.; Iglesia, E. *J. Phys. Chem. B* **2001**, *105*, 3928.
(10) Wang, D.; Lunsford, J. H.; Rosynek, M. P. *Top. Catal.* **1996**, *3*, 289.
(11) Biscardi, J. A.; Meijer, G.; Iglesia, E. *J. Catal.* **1998**, *179*, 192.
(12) Romotowski, T.; Komorek, J.; Mastikhin, V. M. *Pol. J. Chem.* **1995**, *69*, 621.
(13) Wang, L.; Ohnishi, R.; Ichikawa, M. *Catal. Lett.* **1999**, *62*, 29.
(14) Baes, C. F.; Mesmer, P. E. *The Hydrolysis of Cations*; John Wiley and Sons: New York, 1976; p 210.
(15) Borry, R. W.; Kim, Y.-H.; Huffsmith, A.; Reimer, J. A.; Iglesia, E. *J. Phys. Chem. B* **1999**, *103*, 5787.
(16) Clearfield, A. *Proc. 3rd Int. Conf. Mol. Sieves* **1973**.
(17) Chen, H. Y.; Sachtler, W. M. H. *Catal. Lett.* **1998**, *50*, 125.
(18) Asakura, K.; Noguchi, Y.; Iwasawa, Y. *J. Phys. Chem. B* **1999**, *103*, 1051.
(19) Rakshe, B.; Ramaswamy, V. *Stud. Surf. Sci. Catal.* **1998**, *113*, 219.
(20) Rakshe, B.; Ramaswamy, V.; Hegde, S. G.; Vetrivel, R.; Ramaswamy, A. V. *Catal. Lett.* **1997**, *45*, 41.
(21) Rakshe, B.; Ramaswamy, V.; Ramaswamy, A. V. *J. Catal.* **1996**, *163*, 501.
(22) Morey, M. S.; Stucky, G. D.; Schwarz, S.; Froba, M. *J. Phys. Chem. B* **1999**, *103*, 2037.
(23) Yoshida, H.; Chaskar, M. G.; Kato, Y.; Hattori, T. *J. Photochem. Photobiol. A: Chem.* **2003**, *160*, 47.

10.1021/cm060467u CCC: $37.00 © 2007 American Chemical Society
Published on Web 03/10/2007

of $ZrOCl_2$ onto ZSM-5 catalyzed *m*-xylene ammoxidation.[12]

Here, we describe nonaqueous exchange protocols and robust structural assessment strategies to form and characterize Zr^{4+}-oxo species for a range of Zr/Al (0−0.5) ratios in H-ZSM5. Chemical and spectroscopic characterization methods showed that Zr^{4+}-oxo species form $(O{=}Zr{-}O{-}Zr{=}O)^{2+}$ cations by replacing two H^+ at vicinal Al sites; the formation of these species resemble those reported earlier for W, Fe, and V species grafted onto H-ZSM5 using metal-chloride or oxychloride exchange precursors.[9,17,24−26]

2. Experimental Methods

2.1. Synthesis of Zr-ZSM5 Materials. H-ZSM5 was prepared from NH_4-ZSM5 (7−8 g; AlSiPenta, Si/Al = 12.5; <0.03 wt % Na) by treating in flowing dry air (1.67 $cm^3\ s^{-1}\ g^{-1}$, Airgas, 99.999%) while heating to 623 K at 0.05 K s^{-1} and holding at 623 K for 3 h to remove adsorbed H_2O. The temperature was then increased to 773 K at 0.017 K s^{-1} and the sample held at 773 K for 5 h to convert NH_4-ZSM5 into its H-form. The silanol content, reported previously,[24] represented 8% of all the OH groups in H-ZSM5.

Zr-ZSM5 was prepared from $ZrCl_4$ and H-ZSM5 using anhydrous exchange methods previously reported for the synthesis of W-oxo species via grafting of $WCl_{6(g)}$ onto H-ZSM5.[9] The synthesis was carried out in a Schlenk line capable of a dynamic vacuum of 0.13 Pa and equipped with a mechanical pump (Welch 1405) and a liquid N_2 trap. H-ZSM5 (2 g) was treated in vacuum at 573 K for 1 h to remove adsorbed water. Anhydrous $ZrCl_4$ powder (Aldrich, 99.9+%) was isolated from H-ZSM5 during dehydration by a valve; the $ZrCl_4$ and H-ZSM5 were combined after H-ZSM5 dehydration and the resulting $ZrCl_4$/H-ZSM5 physical mixture was sealed within an ampule under vacuum, agitated in a sonicator for 0.1 h to mix the components, and then heated to 650 K at 0.17 K s^{-1} and held at 650 K for 5 h.

The contents of this ampule (in 0.2−0.5 g batches) were transferred into a quartz cell and heated to 373 K at 0.017 K s^{-1} in 1 $cm^3\ s^{-1}$ He (Praxair, 99.999%). The flow was then switched to a 20% O_2/He stream (1 $cm^3\ s^{-1}$; Praxair, 99.999%) contacted with liquid water held in a saturator at 273 K to introduce 0.5 kPa H_2O. The sample temperature was increased to 623 K at 0.17 K s^{-1} and held at 623 K for 0.5 h. The saturator was then bypassed and the sample treated in dry 20% O_2/He (Praxair, 99.999%) while increasing the temperature to 973 K at 0.017 K s^{-1} and holding at 973 K for 1 h. The residual Cl content in $ZrCl_x$-ZSM5 was measured from the amount of HCl evolved (by mass spectrometry, 36 amu) during contact with the H_2O-containing stream. The mass spectrometer response factor was determined by hydrolysis of anhydrous $ZrCl_4$ powders with 20% O_2/He containing 0.5 kPa H_2O while heating the sample to 973 K at 0.17 K s^{-1}. H_2O (18 amu), H_2 (2 amu), and Cl_2 (70−74 amu) were detected by mass spectrometry (MKS, Minilab) with a time resolution of 2 s.

2.2. Isotopic Titration of Residual OH Groups with D_2. Samples (0.2 g) were treated at 773 K in flowing dry air (1 $cm^3\ s^{-1}$; Praxair, 99.999%), cooled rapidly to ambient temperature, and treated in He before contacting them with D_2(5%)/Ar (4.2 $cm^3\ s^{-1}\ g^{-1}$) as the temperature was increased to 973 K at 0.17 K s^{-1} and held for 1 h.[27] The number of OH groups was measured from the amounts of HD and H_2 formed and also from the amount of D_2 consumed. The response factors for H_2 and D_2 were determined from mixtures of known composition, while that for HD (3 amu) was obtained equilibrating H_2-D_2 mixtures on a Pt/ZrO_2 catalyst at 773 K.

2.3. X-ray Diffraction. X-ray diffraction patterns were measured with a Siemens diffractometer (Model D500) and Cu Kα radiation (0.15418 nm wavelength) using powders (0.03 g) ground with KCl (0.03 g) and uniformly spread with Vaseline onto a glass slide. Diffraction data were collected for 2Θ angles of 20−35° at 0.02° intervals with a 40 s hold. KCl was used as an internal standard for angles (2Θ = 28.341°) and intensities. Lattice parameters were obtained by structural refinement after background subtraction using EXPGUI[28,29] and Al-free ZSM-5 structures (silicalite; monoclinic, $P2_1/c$, a = 19.879, b = 20.107, c = 13.369, β = 90.67°).

2.4. Infrared and Raman Spectroscopies. Infrared spectra were measured in transmission mode (Mattson RS 10000) using sample wafers (15 mg cm^{-2}) treated at 673 K in dry air (0.8 $cm^3\ s^{-1}$; Praxair, 99.999%) for 1 h within a cell sealed with CaF_2 windows. Spectra were measured at 673 K with a 2 cm^{-1} resolution using 1000 scans. Infrared band intensities were divided by the intensity of framework overtone bands (1730−2100 cm^{-1}) for H-ZSM5.

Raman spectra were measured with a HoloLab 5000 Research Raman Spectrometer (Kaiser Optical Systems, Inc.) using a 532 nm laser. Hydrocarbons adsorbed on ZSM-5 from ambient air dehydrogenate during thermal treatment to form unsaturated hydrocarbons, which fluorescing during laser irradiation. These residues were removed before measuring Raman spectra by heating Zr-ZSM5 (after exchange and hydrolysis) to 1023 K at 0.17 K s^{-1} in dry air (1.7 $cm^3\ s^{-1}$, Praxair, 99.999%) and holding at 1023 K for 0.1 h. Zeolites were transferred to the Raman cell after cooling and then heated to 823 K at 0.17 K s^{-1} in dry air (1 $cm^3\ s^{-1}$, Praxair, 99.999%) to remove any H_2O adsorbed during transfer. Spectra were measured at 298 K using 20 scans each acquired for 20 s while rotating samples at 7 Hz to avoid local heating by the incident laser.

2.5. Nuclear Magnetic Resonance Spectroscopy. ^{27}Al nuclear magnetic resonance was measured with magic angle spinning (NMR-MAS) using a Bruker AV-500 (11.7 T) spectrometer. Spectra were recorded at 130.3 MHz with a spinning rate of 14 kHz using a single 9° pulse (1.22 μs), a 1 s recycle delay, 3600 scans, and a sweep width of 500 kHz. Chemical shifts are reported relative to those in a 1 M $Al(NO_3)_3$ aqueous solution.

2.6. Density Functional Theory. Bond lengths and angles of Si−O−M (M = Si, Al, or Zr) in MFI zeolites were estimated using density functional theory (DFT) with Gaussian 03[30] to optimize silicalite-1 structures. Silicalite-1 was represented using the T-12

(24) Lacheen, H. S.; Iglesia, E. *J. Phys. Chem. B* **2006**, *110*, 5462.
(25) Lacheen, H. S.; Iglesia, E. *Phys. Chem. Chem. Phys.* **2005**, *7*, 538.
(26) Whittington, B. I.; Anderson, J. R. *J. Phys. Chem.* **1991**, *95*, 3306.
(27) Hall, W. K.; Leftin, H.; Cheselke, F.; O'Reilly, D. E. *J. Catal.* **1963**, *2*, 506.
(28) Toby, B. H. *J. Appl. Crystallogr.* **2001**, *34*, 210.
(29) Larson, A. C.; Von Dreele, R. B. *Gen. Structure Analysis Systems (GSAS)*; Los Alamos National Laboratory Report LAUR 86-748; Los Alamos National Laboratory: Los Alamos, NM, 2000.
(30) Frisch, M. J.; Trucks, G. W.; Schlegel, H. B.; Scuseria, G. E.; Robb, M. A.; Cheeseman, J. R.; Montgomery, J. A., Jr., Vreven, T.; Kudin, K. N.; Burant, J. C.; Millam, J. M.; Iyengar, S. S.; Tomasi, J.; Barone, V.; Mennucci, B.; Cossi, M.; Scalmani, G.; Rega, N.; Petersson, G. A.; Nakatsuji, H.; Hada, M.; Ehara, M.; Toyota, K.; Fukuda, R.; Hasegawa, J.; Ishida, M.; Nakajima, T.; Honda, Y.; Kitao, O.; Nakai, H.; Klene, M.; Li, X.; Knox, J. E.; Hratchian, H. P.; Cross, J. B.; Adamo, C.; Jaramillo, J.; Gomperts, R.; Stratmann, R. E.; Yazyev, O.; Austin, A. J.; Cammi, R.; Pomelli, C.; Ochterski, J. W.; Ayala, P. Y.; Morokuma, K.; Voth, G. A.; Salvador, P.; Dannenberg, J. J.; Zakrzewski, V. G.; Dapprich, S.; Daniels, A. D.; Strain, M. C.; Farkas, O.; Malick, D. K.; Rabuck, A. D.; Raghavachari, K.; Foresman, J. B.; Ortiz, J. V.; Cui, Q.; Baboul, A. G.; Clifford, S.; Cioslowski, J.; Stefanov, B. B.; Liu, G.; Liashenko, A.; Piskorz, P.; Komaromi, I.; Martin, R. L.; Fox, D. J.; Keith, T.; Al-Laham, M. A.; Peng, C. Y.; Nanayakkara, A.; Challacombe, M.; Gill, P. M. W.; Johnson, B.; Chen, W.; Wong, M. W.; Gonzalez, C.; Pople, J. A. *Gaussian 03*, Revision B.04; Gaussian, Inc.: Pittsburgh PA, 2003.

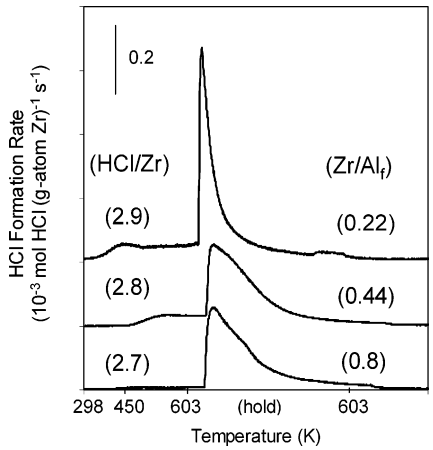

Figure 1. HCl formation rate during exposure of $ZrCl_x$-ZSM5 ($0 < Zr < 0.8$, $Si/Al_f = 13.4$) to 1 cm^3 s^{-1} 20 kPa O_2/0.5 kPa H_2O/80 kPa He after exchange of H-ZSM5 with $ZrCl_4$ at 650 K for 4 h. H-ZSM5 was dehydrated prior to contacting with anhydrous $ZrCl_4$. Values in parentheses represent the integrated mol of HCl per mol of Zr (HCl/Zr) for different Zr to Al_f ratios (Zr/Al_f) in Zr-ZSM5.

site in a 5T cluster (a T-site is a tetrahedral site).[31] Terminal T-sites were bonded with hydrogen ($-SiH_3$) and fixed. A hybrid Becke's exchange functional[32] with the Lee, Yang, and Parr correlation functional[33] (B3LYP) was used for electronic structure calculations, and a 6-31G(d) basis set[34] was used to add polarized character to all atoms except hydrogen.

3. Results and Discussion

HCl evolves during hydrolysis of $ZrCl_x$-ZSM5 as a single peak at all Zr/Al_f (Al_f: framework Al) ratios (Figure 1). Samples with Zr/Al_f ratios of 0.44 and 0.8 formed HCl at higher temperatures than samples with a Zr/Al_f ratio of 0.22, apparently because some of the evolved HCl re-adsorbs as HCl concentrations increase with increasing Zr content. The amount of HCl evolved was 2.8 ± 0.1 HCl/Zr for all samples, indicating that $ZrCl_4$/H-ZSM5 mixtures led to $ZrCl_4$ reactions with H^+ at 650 K to form HCl and $ZrCl_3^+$; these data are consistent with an initial exchange stoichiometry of one Zr per OH group.

X-ray diffraction patterns after removal of chloride from Zr-ZSM5 resembled those for the parent zeolite (Figure 2), indicating that zeolite structures were preserved during contact with $ZrCl_4$ and subsequent hydrolysis. The unit cell volume (UCV) in aluminosilicates is sensitive to Al framework content;[35] thus, changes in lattice constants can be used to detect Al removal or Zr incorporation during sublimation of $ZrCl_4$ and subsequent hydrolysis. Lattice cell volumes (Table 1) in H-ZSM5 (6.7 Al/u.c.) were higher than those in silicalite (the pure SiO_2 form of ZSM-5; 5338 Å^3) by 45 Å,^{3} as also reported by others.[35] The presence of one Zr per unit cell in silicalite increased cell volumes by 40 Å^3 and higher Zr contents led to a proportional increase in unit cell volume.[20] Such changes reflect a concomitant increase in M−O (M = framework Si, Al, or Zr) bond lengths.[35] We have confirmed these conclusions using density functional theory calculations of M−O bond lengths in silicalite as various cations are inserted into T-12 sites within a theoretical 5T cluster (Table 2). M−O distances are longer for Zr−O (0.188 nm) than for Al−O (0.172 nm) bonds, consistent with the trend in volume expansions observed in experiments.[20] Distances of Zr−O bonds of 0.194 nm in Zr-silicalite-2, measured using EXAFS, have also been reported by Ramaswamy et al.[36] In view of these estimates, X-ray diffraction with structural refinement was used here to detect any incorporation of Zr into the ZSM-5 framework during exchange.

Dealumination and Zr incorporation into framework positions may occur during contact with $ZrCl_4$, by analogy with reported zeolite dealumination protocols using $SiCl_4$.[37] Such processes would increase the unit cell volume, based on the data shown in Table 2. The replacement of 1 Al with Zr in each unit cell ($Zr/Al_f = 0.15$) would increase unit cell volumes by 33 Å.^{3} Cell volumes measured from diffractograms were 5387 ± 4 Å^3 for all Zr-ZSM5 in our study; these values are identical, within experimental accuracy, to those for the parent H-ZSM5 (5383.5 Å^3), and inconsistent with any Al extraction or Zr incorporation during exchange. Thus, our $ZrCl_4$ grafting protocols place Zr-oxo species onto the exchange site without detectable replacement of framework Al atoms.

The local structure of Al atoms in Zr-ZSM5 and H-ZSM5 was also probed using ^{27}Al NMR-MAS (Figure 3). ^{29}Si NMR did not provide conclusive evidence for Zr framework incorporation because chemical shifts arising from framework Si−O−Al cannot be distinguished from those for Si−O−Zr structures in H-ZSM5. ^{27}Al NMR spectra showed two lines with chemical shifts at 54 and 0 ppm for tetrahedral framework Al and octahedral extraframework Al, respectively. The line at 54 ppm became broader after Zr exchange and acquired a shoulder at lower chemical shifts; both trends continue as Zr/Al_f ratios increased. The line at 0 ppm also broadened but was similar in intensity for all samples. For samples with $Zr/Al_f < 0.8$, ^{27}Al NMR spectra reflect contributions from Al atoms interacting with H^+ and with exchanged Zr^{4+}-oxo cations, which lead to nonuniform Al coordinations and broader Al NMR features, a reflection of unresolved multiple lines shifted slightly from those for Al atoms interacting with protons.

Residual OH groups after $ZrCl_4$(g) contact with H-ZSM5 and subsequent hydrolysis and dehydration were detected from the amount of HD (and H_2) formed by D_2 reactions with OH (Figure 4). The parent H-ZSM5 gave 1.07 ± 0.05 OH/Al_f, as expected from charge balance requirements (1:1 H:Al) and the presence of trace silanols. The number of residual OH groups decreased linearly with increasing Zr/Al_f ratio; the corresponding slope gives 1.2 ± 0.1 OH removed per Zr atom for Zr/Al_f ratios below 0.5, consistent with an exchange stoichiometry near unity (Table 3). This

(31) van Koningsveld, H.; van Bekkum, H.; Jansen, J. C. *Acta Crystallogr., Sect. B* **1987**, *64*, 127.
(32) Becke, A. D. *J. Chem. Phys.* **1993**, *98*, 5648.
(33) Lee, C.; Yang, W.; Parr, R. G. *Phys. Rev. B* **1988**, *37*, 785.
(34) Hariharan, P. C.; Pople, J. A. *Theor. Chim. Acta* **1973**, *28*, 213.
(35) Meyers, B. L.; Ely, S. R.; Kutz, N. A.; Kaduk, J. A. *J. Catal.* **1985**, *91*, 352.
(36) Ramaswamy, V.; Tripathi, B.; Srinivas, D.; Ramaswamy, A. V.; Cattaneo, R.; Prins, R. *J. Catal.* **2001**, *200*, 250.
(37) Klinowski, J.; Thomas, J. M.; Anderson, M. W.; Fyfe, C. A.; Gobbi, G. C. *Zeolites* **1982**, *3*, 5.

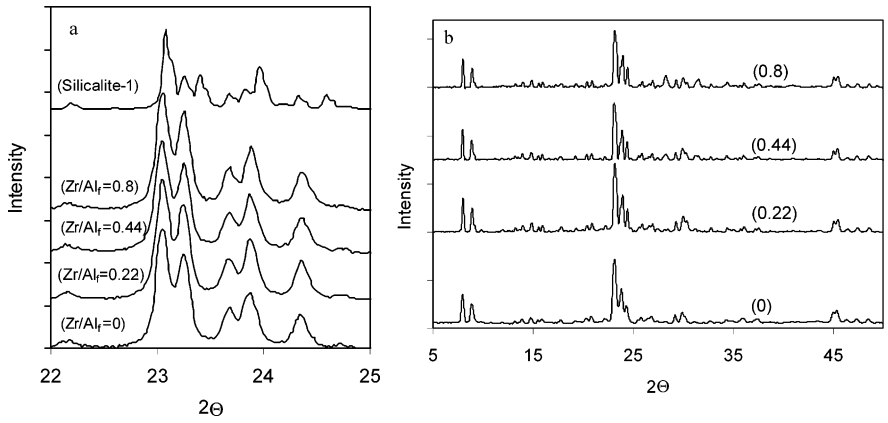

Figure 2. X-ray diffraction patterns of Zr-ZSM5 ($0 < Zr < 0.8$, $Si/Al_f = 13.4$) between 2Θ of (a) 22−25 and (b) 5−50.

Table 1. Unit Cell Parameters for Zr-ZSM5 ($0 < Zr/Al_f < 0.8$, $Si/Al_f = 13.4$)[a]

	lattice dimensions (Å)				
Zr/Al_f	*a*	*b*	*c*	β (deg)	UCV (Å^3)
0	19.85(3)	20.18(7)	13.43(2)	90.54(2)	5383.(5)
0.22	19.87(1)	20.20(0)	13.43(1)	90.56(2)	5391.(0)
0.44	19.94(3)	20.20(5)	13.36(4)	90.51(8)	5385.(2)
0.8	19.88(7)	20.15(2)	13.43(5)	90.57(9)	5384.(4)

[a] Crystal parameters were refined from silicalite-1 using KCl as internal standard. Diffraction patterns were fit between 2Θ angles of 20° and 35°.

Table 2. Average Calculated M−O Distance and Experimental Change in Unit Cell Volume (ΔUCV) per Metal Content for Framework Si, Al, and Zr Atoms in ZSM-5 Structures[a]

metal	average M−O distance (Å)	ΔUCV/metal (Å^3 M^{-1})
Si	1.61	
Al	1.72	7
Zr	1.88	40

[a] Average M−O distances were calculated using density functional theory simulations of the T-12 site in a 5T ZSM-5 cluster.

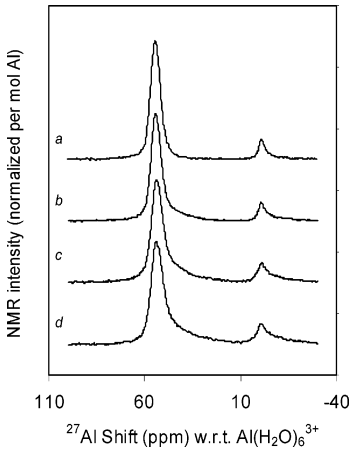

Figure 3. ^{27}Al MAS NMR spectra of H-ZSM5 and Zr-ZSM5. (a) H-ZSM5 ($Si/Al_f = 13.4$); (b) $Zr/Al_f = 0.12$; (c) $Zr/Al_f = 0.44$; (d) $Zr/Al_f = 0.8$.

exchange stoichiometry is lower (0.78 OH/Zr) for the sample with the higher Zr/Al_f ratio (0.8).

Infrared spectra of OH stretches gave trends similar to D_2−OH exchange experiments with Zr/Al_f ratio (Figure 5). The intensity of the band at ~3600 cm^{-1}, corresponding to acidic OH groups (the weak band at 3740 cm^{-1} arises from silanols), decreased with increasing Zr/Al_f ratios. Figure 6 shows $\Delta(OH)/Al_f$ values from D_2−OH and infrared data as

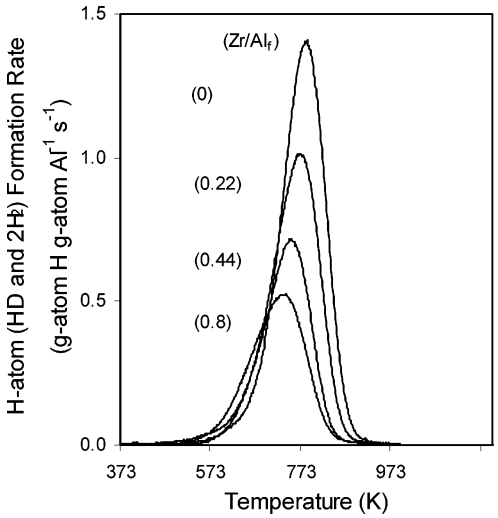

Figure 4. Formation rate of HD and $2H_2$ vs temperature on H-ZSM5 ($Si/Al_f = 13.4$) and Zr-ZSM5 ($Zr/Al_f = 0.2-0.8$) during treatment in 5% D_2/Ar with a heating rate of 0.17 K s^{-1}.

Table 3. Change in Hydroxyl Content per Al or Zr Atom in Zr-ZSM5 ($0 < Zr < 0.8$) (Δ(OH)/Zr) Measured Using D_2−OH Exchange and Infrared Hydroxyl Stretching Bands

	D_2−OH exchange		infrared	
Zr/Al_f	$\Delta(OH)/Al_f$[a]	Δ(OH)/Zr	$\Delta(OH)/Al_f$[b]	Δ(OH)/Zr
0	0		0	
0.12	0.15	1.27	0.20	1.7
0.22	0.26	1.19		
0.44	0.46	1.05	0.53	1.2
0.8	0.61	0.76	0.55	0.7

[a] Amount of OH per framework Al (Al_f) in the sample is calculated by HD formation; estimated uncertainty is 0.05 OH/Al_f. [b] Area of band at 3600 cm^{-1} for H-ZSM5 normalized; estimated uncertainty is 0.1 OH/Al_f.

a function of Zr/Al_f ratio. These two independent sets of data agree within their respective accuracies and give an exchange stoichiometry of 1.2 ± 0.1 Δ(OH)/Zr for Zr/Al_f ratios lower than 0.5. For the sample with a higher Zr/Al_f ratio (0.8), the infrared spectra gives a ΔOH/Zr ratio of 0.7 ± 0.1, which also resembles the value obtained from isotopic exchange data.

Charge neutrality requires that exchanged Zr^{4+}-oxo species be present as either ZrO^{2+} monomers (Chart 1, Structure I) or $Zr_2O_3^{2+}$ dimers (Chart 1, Structure II), each interacting with two next-nearest neighbor Al sites. Only dimers are consistent with the exchange stoichiometry measured for Zr/Al_f ratios below 0.5 (1.2 ± 0.1 Δ(OH)/Zr). Experimental

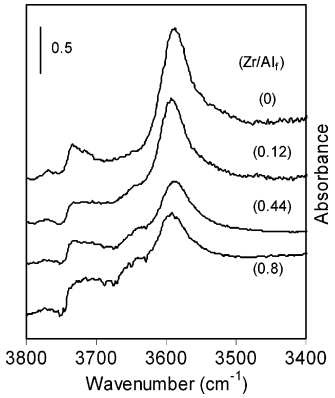

Figure 5. Infrared spectra for H-ZSM5 (Si/Al$_f$ = 13.4) and Zr-ZSM5 (Zr/Al$_f$ = 0.2−0.8) at 673 K in dry air. Fourier-transformed spectra were recorded in transmission mode using 1000 scans. Spectral intensities were normalized by zeolite framework overtone bands between 1730 and 2100 cm^{-1}.

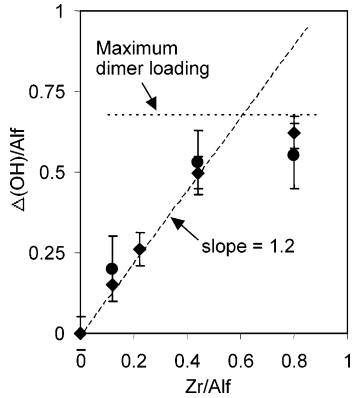

Figure 6. Change in OH per Al$_f$ (framework Al) as a function of Zr loading on H-ZSM5 (Si/Al$_f$ = 13.4) measured using infrared spectroscopy (●) and D_2−OH exchange (◆). Zr-ZSM5 samples were prepared by vapor exchange of $ZrCl_4$ onto dehydrated H-ZSM5 at 700 K for 5 h and hydrolyzed using 1 kPa H_2O in 20% O_2/He at 625 K. The dashed line represents a linear least-square regression for the Zr/Al$_f$ < 0.5. The dotted line represents the maximum Zr/Al$_f$ dimer loading calculated from data from ref 38 and 39 and assuming a maximum 0.85 nm Al−Al distance.

Chart 1

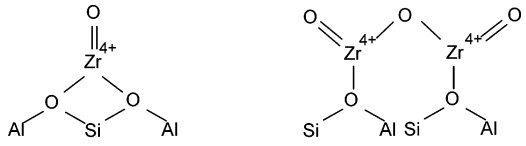

ΔOH/Zr values are slightly above unity, apparently because minority monomer species form at very low Zr contents, for which vicinal $ZrO(OH)^+$, required to form $Zr_2O_3^{2+}$ dimers, are scarce. As a result, $ZrO(OH)^+$ condenses instead with neighboring OH groups to form less stable ZrO^{2+} monomers bridging two Al sites. Al sites that lack an Al atom within 0.92 nm cannot form either monomer or dimer structures and must remain as $ZrO(OH)^+$; they could de-anchor in the presence of trace moisture to exchange with another OH or migrate to external surfaces and form extraframework ZrO_2. We have examined the latter possibility using Raman spectra, which are very sensitive to crystalline ZrO_2.

At Zr/Al$_f$ ratios above 0.5, the exchange stoichiometry (ΔOH/Zr) becomes smaller than unity (Figure 6). Prevalent dimer structures $(O{=}Zr{-}O{-}Zr{=}O)^{2+}$ and minority ZrO_2^+ monomers both require site pairs with Al−Al distances consistent with the size of Zr-oxo structures; clearly, this requirement cannot be satisfied by all Al sites in ZSM-5. Random and thermodynamic arrangements of Al atoms can be used to estimate radial distribution functions in ZSM-5.[38,39] These results, taken together with the expected dimensions of $(O{-}Zr{-}\mu O{-}Zr{-}O)^{2+}$ structures estimated from Zr−O bond lengths (0.20−0.24 nm) measured by neutron diffraction,[40] can be used to estimate the number of Al−Al pairs that can interact with Zr-oxo dimers and thus the maximum Zr/Al$_f$ ratios for which dimers can form. Zr-oxo dimers require Al−Al distances smaller than 0.92 nm; the fraction of Al atoms in Al−Al pairs satisfying this requirement (from calculated radial structure functions[38]) for a Si/Al$_f$ ratio of 12 was 0.34 dimers/Al$_f$, corresponding to a Zr/Al$_f$ ratio of 0.68 for the maximum Zr content at which dimers can form as the sole Zr-oxo structure. This estimate is slightly larger than the highest Δ(OH)/Al$_f$ exchange ratio (0.55−0.61 ± 0.05) measured from D_2−OH exchange and infrared spectra (Table 3). These slight differences may reflect small differences in Al$_f$ content between our ZSM-5 (Si/Al$_f$ = 13.4) and that in the reported simulations (Si/Al$_f$ = 12).[38] We conclude that Zr atoms exceeding those required for a Zr/Al$_f$ ratio of 0.68 cannot form either structure I or structure II; thus, $ZrO(OH)^+$ species de-anchor during hydrolysis or dehydroxylation to form ZrO_2 nuclei at extraframework positions probably at external surfaces.

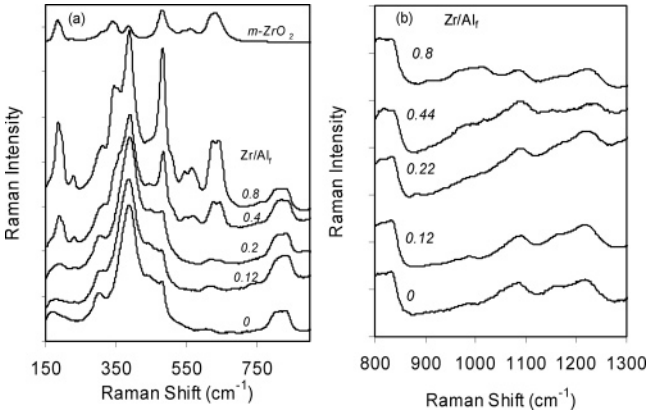

Figure 7. Raman spectra of H-ZSM-5, Zr-ZSM5, and monoclinic ZrO_2 materials recorded at 298 K after ex situ treatment at 1023 K in dry air followed by in situ dehydration at 823 K in dry air. Numbers above each spectrum represent the Zr/Al$_f$ ratios. Spectra were normalized to framework T−O−T stretches at 850 cm^{-1} with (a) displaying the spectra from 150 to 850 cm^{-1} and (b) on a smaller scale displaying spectra from 800 to 1300 cm^{-1}.

Next we examine Raman spectra of Zr-ZSM5 samples for evidence of Zr-oxo species present as monomers, dimers, or crystalline ZrO_2. Figure 7 shows Raman vibrational spectra for Zr-ZSM5, H-ZSM5, and monoclinic ZrO_2. Zr-ZSM5 samples gave Raman bands between 960 and 1030 cm^{-1} (Figure 7b), absent in H-ZSM5. These bands are broader but similar in frequency to Zr−O−Si bands in crystalline $Zr_xSi_{1-x}O_2$ at 940−960 cm^{-1}.[19−22] Zr−O modes in Zr^{4+}-oxo species on ZSM-5 are expected to be weak because of the

(38) Rice, M. J.; Chakraborty, A. K.; Bell, A. T. *J. Catal.* **1999**, *186*, 222.
(39) Rice, M. J.; Chakraborty, A. K.; Bell, A. T. *J. Catal.* **2000**, *194*, 278.
(40) Howard, C. J.; Hill, R. J.; Reichert, B. E. *Acta Crystallogr., Sect. B* **1988**, *44*, 116.

nonuniform binding sites that stabilize grafted isolated structures. Structure II contains Zr−O−Si, Zr−O−Al, and Zr═O linkages, which would be Raman-active because of the C_{2V} symmetry of $Zr_2O_3^{2+}$ dimers, and would give bands at ~1000 cm^{-1}, as found in zirconyl salts[41] and in analogous Mo^{6+} and V^{5+} oxo-dimers exchanged onto H-ZSM5.[24,42] The observed bands in the spectra for Zr-ZSM5 were too small for a conclusive spectral assignment, especially in Zr-ZSM5 with Zr/Al_f ratios below 0.44; therefore, these spectra cannot provide definitive evidence for structures I or II.

Crystalline ZrO_2 gives no detectable bands above 900 cm^{-1} for any of its stable monoclinic, tetragonal, or cubic phases.[43−47] Below 800 cm^{-1} (Figure 7a), the Raman spectra for Zr-ZSM5 samples with Zr/Al_f ratios of 0.12 and 0.22 are identical to those for unexchanged H-ZSM5. Monoclinic ZrO_2 (*m*-ZrO_2) bands were evident on Zr-ZSM5 samples with Zr/Al_f ratios of 0.44 and 0.8, as also detected by X-ray diffraction (not shown in Figure 2). X-ray diffraction patterns showed evidence of crystalline *m*-ZrO_2 (with intensity calibrated from *m*-ZrO_2/H-ZSM5 mixtures), present in Zr-ZSM5 at 15% and 25% of total Zr for Zr/Al_f ratios of 0.44 and 0.8, respectively. The amount of ZrO_2 formed in the 0.8 Zr/Al_f sample (corresponding to 0.2 Zr/Al_f) is somewhat higher than predicted from the deviations from a unity exchange stoichiometry in these samples (0.12 ± 0.05 Zr/Al_f assuming a maximum Zr/Al_f ratio of 0.68 for dimers). This small discrepancy reflects the formation of some ZrO^{2+} monomers, which require two Al sites per Zr, and thus decrease the maximum Zr/Al_f dimer ratio. The presence of ZrO_2^{+} monomers is also evident from the measured exchanged stoichiometry (1.2 ± 0.1 ΔOH/Zr), which is slightly higher than that expected from dimers.

4. Conclusions

Zr^{4+} cations were grafted selectively onto exchange sites in H-ZSM5 using $ZrCl_4$ vapor under anhydrous conditions. Structures with $ZrCl_3^{+}$ stoichiometry formed initially and their Cl ligands were removed by subsequent hydrolysis at 623 K. In samples with low Zr/Al_f ratios, each Zr^{4+} cation replaced 1.2 ± 0.1 OH by forming predominantly $Zr_2O_3^{2+}$ dimers. At higher Zr/Al_f ratios, the change in OH content per Zr approached a constant value of ~0.6 as a result of the limited number of Al−Al pairs. X-ray diffraction and ^{27}Al MAS NMR spectra showed that the zeolite structure remains intact during exposure to $ZrCl_4$(g) and subsequent thermal treatments and that Zr was not incorporated into the zeolite framework.

Acknowledgment. The authors acknowledge financial support from the Ford Foundation through the Ford Catalysis Fellowship administered by the Berkeley Catalysis Center. Drs. Stacey Zones, Allen Burton, and C. Y. Chen (Chevron Corp.) are also acknowledged for their technical guidance in the simulation and characterization of the structure of the materials reported here.

CM060467U

(41) Dehnicke, K.; Weidlein, J. *Angew. Chem., Int. Ed.* **1966**, *5*, 1041.
(42) Li, W.; Meitzner, G. D.; Borry, R. W.; Iglesia, E. *J. Catal.* **2000**, *191*, 373.
(43) Adams, R. C.; Xu, L.; Moller, K.; Bein, T.; Delgass, W. N. *Catal. Today* **1997**, *33*, 263.
(44) Meijun, L.; Feng, Z.; Xiong, G.; Xin, Q.; Li, C. *J. Phys. Chem.* **2001**, *105*, 8107.
(45) Kourouklis, G. A. *J. Am. Ceram. Soc.* **1991**, *74*, 520.
(46) Phillippi, C. M.; Mazdiyasni, K. S. *J. Am. Ceram. Soc.* **1971**, *54*, 254.
(47) Ishigame, M.; Sakuri, T. *J. Am. Ceram. Soc.* **1977**, *60*, 367.